OPTOELECTRONICS AND ADVANCED MATERIALS – RAPID COMMUNICATIONS Vol. 6, No. 3-4, March - April 2012, p. 427 - 433

Efficient green fluorescence and upconversion emissions from Er^{3+} ions in CdS sol-gel silica glass

PANKAJ DUTTA
Laser and Spectroscopy laboratory, Department of Physics, Dibrugarh University, Dibrugarh -786 004, Assam, India

Er^{3+} ions doped in CdS silica glasses were prepared by sol-gel route. Absorption and photoluminescence spectra of the glasses were analyzed in the light of the Judd-Ofelt theory. Spectroscopic analysis of the multiphoton processes in the glasses was carried out by monitoring the upconversion luminescence. The study reveals the potential of the present glass for the $^4S_{3/2} \rightarrow {}^4I_{15/2}$ and $^2H_{11/2} \rightarrow {}^4I_{15/2}$ Erbium lasing transitions.

(Received January 11, 2012; accepted April 11, 2012)

Keywords: Judd Ofelt Parameters, Photoluminescence, Upconversion, Rare-Earth

1. Introduction

Recently there has been renewed interest in rare earth (RE) doped fibers and waveguides because of their applications in amplifiers and lasers. The optical properties of RE ions trapped in host lattices continue to be an attractive research theme in view of both fundamental and technological importance [1]. As a branch of visible luminescence, upconversion luminescence of RE ions has been catching more and more attentions [2, 3]. The interest in upconversion emission of RE doped materials has been increased because of the search for all solid compact laser devices operating in the visible region and the availability of powerful near infrared laser diodes. In the development of RE doped optical devices, host glass matrix is a very important factor to be considered. The choice of suitable glass former and glass modifier systems helps in tailoring glass matrix to meet the specific requirements. Accordingly, the study of sol-gel derived RE activated materials continue to be an attractive research area because of the flexibility provided by the process (sol-gel) in choice of host constituents and concentrations that influence the luminescence properties of RE transitions. Among the RE ions that exhibit fluorescence, Er^{3+} is the most popular as well as one of the most efficient ions that have been observed in various glass hosts [4, 5]. Though the silica glasses possess high chemical durability, better thermal stability, superior chemical resistance and are optically transparent at the excitation and lasing wavelengths [6], they are not much studied for luminescence and upconversion applications owing to their higher phonon energies [7]. It is well established that the radiative parameters associated with luminescence transitions of lanthanide (Ln^{3+}) ions in glasses are highly sensitive even for small changes in the chemical environment. The transition probabilities for emission from Ln^{3+} ions are expected to increase with increase in covalency that depends upon the network forming ions. Network modifiers also change the local environment of Ln^{3+} ions to some extent [6, 8].

Both direct and indirect band-gap semiconductors could be a good choice as sensitizing centers since their excitation cross sections are very high due to the efficient band to band absorptions [9]. RE doped glass matrices containing semiconductor quantum dots have been prepared by the sol-gel method by various authors [10-13]. Semiconductor CdS has been used as co-dopant by many workers as its presence can lead to increase in luminescence intensity from RE centers owing to the energy transfer from the CdS particles to the RE ions [14, 15]. J. Mu [16] et al. had reported an increase in emission intensity of Eu^{3+}- SiO_2 network when the CdS particles were introduced into the network

Keeping in mind the important physical and chemical properties of the silica glasses, we have been studying the optical properties of the silica glasses with different RE ions as dopants. Recently, we have reported the green upconversion fluorescence around 532 and 549nm from Er^{3+} ions [17] and green and blue upconversions from Ho^{3+} singly doped and Ho^{3+}/Yb^{3+} co-doped ions in $Al(NO_3)_3$-SiO_2 glasses [18]. In this paper, we report the fabrication and characterization of Er^{3+}doped with CdS silica glass by sol-gel route. The optical absorption, the Judd Ofelt (J.O) parameters [19, 20], the spontaneous transition probabilities, excited state lifetimes and the fluorescence branching ratios have been calculated from the observed absorption and photoluminescence spectra. Intense green upconversion fluorescence bands around 533, 549 nm and red band around 626nm were observed under 800 nm excitation. The mechanisms involved in the upconversion process viz. excited state absorption (ESA), cross relaxation (CR) etc. on Er^{3+} upconversion emissions with emphasis on green and red lasing transitions are discussed.

2. Experimental details

Er^{3+} singly doped CdS -SiO_2 glasses for the present study were prepared by sol-gel route as explained in earlier paper [18]. Tetraethylorthosilicate (TEOS) (Merck >98%) as organo metallic precursor, methanol (Merck 99%) as solvent and nitric acid (Merck 70%) as catalyst were used together with doubly distilled water in proportion of 16:70:4:10. To this solution, 0.01M Er_2O_3 (Aldrich 99.999%) and 0.01M CdS (Aldrich 99.99%) were added. Dopants in above concentrations were mixed with methanol, nitric acid, doubly distilled water and were stirred by a magnetic stirrer for about 30 minutes. To this solution TEOS was added and the mixture was further stirred for about 1 hour or till gelation begins. The gel was then put in plastic container and dried at room temperature to densify the mass into an amorphous, porous solid matrix called xerogel. Dopants in sol-gel glasses got impregnated into these pores. After about 100 hours the gel shrunk to about half its original volume and solidified. Further densification is accomplished by leaving it to dry at room temperature for 21 days followed by annealing in ambient at 500 °C for two hours to obtain the final glass.

The refractive index (n) of the glass was calculated from the measurement of Brewster's angles using a spectrometer with 632.8 nm He-Ne laser light. Refractive index obtained for the present glass is 1.52. The optical absorption spectrum of Er^{3+} doped in CdS -SiO_2 sol-gel glass was recorded on a Hitachi U-2001 double beam UV/VIS spectrophotometer with spectral resolution 0.1 nm using undoped glass as reference. Photoluminescence and upconversion spectra were recorded by using the excitation wavelengths at 480 and 800nm respectively by a Fluoromax 4P spectrofluorimeter with spectral resolution 1 nm. For both the excitations 150 watt CW xenon lamp was used. All the measurements were done at room temperature.

3. Results and discussions

3.1. Judd Ofelt analysis

The room temperature optical absorption spectrum of Er^{3+} (0.01 M) in CdS -SiO_2 glasses in the region of 300-1000 nm, ascribed to electric dipole (e-d) transitions is shown in Fig. 1. Eleven absorption bands of Er^{3+} for the transitions from $^4I_{15/2}$ ground state to $^4G_{9/2}$, $^4G_{11/2}$, $^2H_{9/2}$, $^4F_{3/2}$, $^4F_{5/2}$, $^4F_{7/2}$, $^2H_{11/2}$, $^4S_{3/2}$, $^4F_{9/2}$, $^4I_{9/2}$ and $^4I_{11/2}$ states respectively, were observed superimposed on the absorption spectrum of CdS. Assignments of the absorption peaks were done by comparing with earlier works [21, 22].

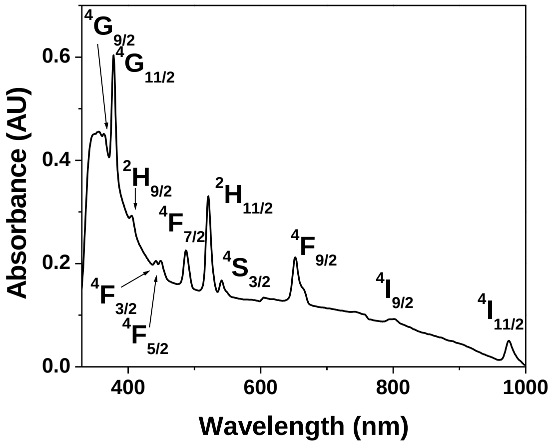

Fig. 1. Optical absorption spectrum for 0.01M Er^{3+} doped CdS -SiO_2 glass.

The experimental oscillator strengths ($f_{\exp}$) of the observed e-d transitions are determined from the relation

$$f_{\exp} = 4.318 \text{ x } 10^{-9} \int \varepsilon(\nu) d\nu \tag{1}$$

where, $\varepsilon(\nu)$ is the molar extinction co-efficient at wave no ν (cm^{-1}) determined from Lambert Beer's law. To determine the Judd Ofelt (J.O.) parameters T_t for t = 2, 4 & 6, oscillator strengths measured experimentally were co-related with its corresponding Judd's [19] expression for oscillator strengths of e-d transitions between initial ΨJ and terminal $\Psi' J'$ states, by

$$f_{cal} = \sum_{t=2.4.6} T_t \nu (\langle \Psi J \| U(t) \| \Psi' J' \rangle)^2 \tag{2}$$

using the least square fit analysis. In equation (2), $U(t)$ is a tensor operator of rank t calculated in an intermediate coupling approximation [23]. Since the values of these operators are essentially independent of hosts, values calculated by Carnall et al [22] for Er^{3+} (aquo) ions are used in these calculations. In the characterization of spectral intensities of the absorption bands, the glass refractive index (n) plays an important role. Therefore, the original J.O. parameters (T_t) are transformed into Ω_t parameters through the following expression,

$$\Omega_t = \frac{3h}{8\pi^2 mc} \frac{9n}{(n^2+2)^2} (2J+1) T_t \tag{3}$$

In equation (3), n is the refractive index of material, $(2J+1)$ is the multiplicity of the lower state, m the mass of the electron while the rest of the symbols have their usual meanings.

The measured experimental ($f_{\exp}$) and calculated theoretical (f_{cal}) oscillator strengths of the observed Er^{3+} transitions in CdS -SiO$_2$ sol-gel glass are compiled in Table 1 along with the J.O. intensity parameters (Ω_t). The values of experimental and theoretical oscillator strengths are in good agreement with an r.m.s. deviation of ± 1.13 × 10^{-6} between them which suggests the reliability of the calculation process. The larger differences observed between the calculated and the experimental values of oscillator strengths for some of the transitions is because of 4f–5d mixing [24] which may contribute to intensities with odd values of t in $\|U(t)\|$ matrix elements which are neglected in the J.O. model.

Table 1. The experimental and theoretical oscillator strengths with Judd Ofelt intensity parameters for Er^{3+} transitions in CdS -SiO$_2$ glass.

Grnd. state	**Exctd. state**	**Energy (cm^{-1})**	**Oscillator Strength (10^{-6})**	
			Calctd. (f_{cal})	**Exptl. (f_{exp})**
$^4I_{15/2}$	$^4G_{9/2}$	27473	0.79	0.61
	$^4G_{11/2}$	26455	13.39	12.01
	$^2H_{9/2}$	24691	0.53	0.32
	$^4F_{3/2}$	22624	0.15	0.31
	$^4F_{5/2}$	22272	0.46	0.66
	$^4F_{7/2}$	20534	3.54	3.48
	$^2H_{11/2}$	19194	5.88	9.07
	$^4S_{3/2}$	18484	0.38	1.02
	$^4F_{9/2}$	15337	3.04	3.04
	$^4I_{9/2}$	12469	0.14	0.48
	$^4I_{11/2}$	10267	0.68	0.71
r.m.s deviation (10^{-6})			1.13	
Ω_2 (10^{-20} cm^2)			5.09	
Ω_4 (10^{-20} cm^2)			4.13	
Ω_6 (10^{-20} cm^2)			4.55	
Ω_4 / Ω_6			0.91	

The J.O. intensity parameters (Ω_t) are important for analysis of local structure and bonding in the vicinity of the RE ions. It is well known that the Ω_2 parameter depends on the structure and is associated with the asymmetry and covalency of the lanthanide sites [25]. The Ω_4 and Ω_6 parameters depend on bulk properties of the host such as viscosity and dielectric property of the medium and are also affected by the vibronic transitions of the RE ions bound to the ligand atoms [26]. Moreover, the values of the J.O. intensity parameters can be used to calculate the spectroscopic quality factor Ω_4/Ω_6, which is critically important in predicting the stimulated emission for the laser active medium [25, 27]. The J.O. intensity parameters obtained for the studied CdS-SiO$_2$ glass were compared with other popular glass hosts and are presented in Table 2. The J.O. intensity parameters for Er^{3+} in pure SiO$_2$ glass were also evaluated and are presented in the table for better understanding.

Table 2. Comparative Judd Ofelt intensity parameters and the spectroscopic quality factors for Er^{3+} in various hosts.

Host Glasses	**Ω_2 (10^{-20} cm^2)**	**Ω_4 (10^{-20} cm^2)**	**Ω_6 (10^{-20} cm^2)**	**Ω_4/Ω_6**	**Reference**
CdS -SiO$_2$	5.09	4.13	4.55	0.91	Present work
(Pure) SiO$_2$	4.24	4.99	4.46	1.12	Present work
Silicate	4.23	1.04	0.61	1.70	[28]
LaF$_3$	1.27	0.28	0.63	0.44	[29]
BaF$_2$	1.048	1.478	1.009	0.68	[29]
Fluoro phosphate	2.91	1.63	1.26	1.29	[30]
Fluoride	2.91	1.27	1.11	1.13	[31]
Tellurite	5.05	1.45	1.22	1.19	[31]
Germanate	4.81	1.41	0.48	2.94	[32]
Phosphate	3.89	1.01	0.55	1.84	[33]
Bismuth	3.86	1.52	1.17	1.30	[33]

Comparatively higher value of Ω_2 parameter for the present glass indicates higher asymmetry and stronger covalent environment between RE and ligand ions in Er^{3+} doped CdS -SiO_2 glass. The result is important since the transition probabilities for emission of Ln^{3+} ions are expected to increase with increase in covalency [6, 8]. Moreover, comparison of the J.O. intensity parameters for the CdS-SiO_2 glass with that of (pure) silica glass reveals the significant modifying effect of CdS on the glass network.

The Ω_4 parameter together with Ω_6 has effect on some transitions of Er^{3+}, such as the $^4S_{3/2} \rightarrow {}^4I_{15/2}$ transition [29], because the spontaneous transitions of $^4S_{3/2}$ state depend only on the Ω_4 and Ω_6 parameters as the reduced matrix elements of the unit tensor $U(2)^2$ is equal to zero (as listed in Table 3). Furthermore, for $^4S_{3/2} \rightarrow {}^4I_{15/2}$ transition, $U(4)^2$ is also equal to zero; but $U(4)^2$ still has contribution on the other branching ratios for the $^4S_{3/2}$ luminescence. Thus the smaller Ω_4 and larger Ω_6 are favorable for the $^4S_{3/2} \rightarrow {}^4I_{15/2}$ luminescence of Er^{3+}. In order to enhance the luminescence intensity of $^4S_{3/2} \rightarrow {}^4I_{15/2}$ in comparison to $^4S_{3/2} \rightarrow {}^4F_{9/2}$, $^4I_{9/2}$, $^4I_{11/2}$ and $^4I_{13/2}$ transitions, one therefore requires $\Omega_4 << \Omega_6$. Therefore, Ω_4/Ω_6 factor becomes critical [34] while measuring the efficiency of the visible laser transition $^4S_{3/2} \rightarrow {}^4I_{15/2}$ of Er^{3+}. Thus, smaller the value of Ω_4/Ω_6, more intense is the relative emission intensity of $^4S_{3/2} \rightarrow {}^4I_{15/2}$ transition. From table II it is seen that the Ω_4/Ω_6 value for the Er^{3+}: CdS -SiO_2 glass is reasonably less among the compared glasses; which indicates that the studied glass will be very proficient for $^4S_{3/2} \rightarrow {}^4I_{15/2}$ Er^{3+} lasing transition.

3.2. Fluorescence emission analysis

The photoluminescence spectrum for the Er^{3+}: CdS -SiO_2 sol-gel glass under 480 nm excitation is shown in Fig. 2. Two emission bands centred at 533 and 549 nm corresponding to the $^4S_{3/2} \rightarrow {}^4I_{15/2}$ and $^2H_{11/2} \rightarrow {}^4I_{15/2}$ Er^{3+} transitions were observed in the studied range. Using the emission spectrum and the values of Ω_t, important radiative parameters for the observed emission transitions were estimated [35].

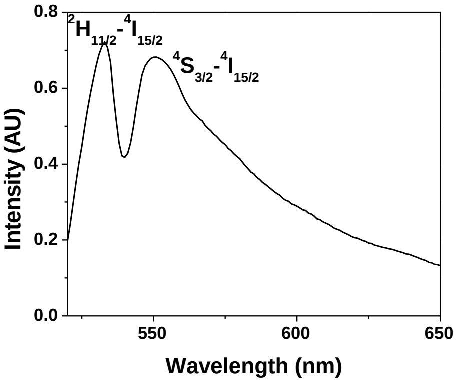

Fig. 2. Photoluminescence spectrum in green region for 0.01M Er^{3+} doped CdS -SiO_2 glass under 480 nm excitation.

The spontaneous emission probability is given by

$$A(\Psi J, \Psi' J') = \frac{64\pi^4 e^2 n(n^2+2)^2}{3h\lambda^3(2J+1)9} \sum_{t=2,4,6} \Omega_t \left|\langle \Psi J \| U(t) \| \Psi' J' \rangle\right|^2 \quad (4)$$

The total spontaneous emission probability for all transitions from this state is

$$A_T = \sum A(\Psi J, \Psi' J') \quad (5)$$

and A_T^{-1} gives the radiative lifetime (τ_{rad}) that determines the rate of depopulation of the given state.

The fluorescence branching ratio of transitions from the initial (ΨJ) to the lower $(\Psi' J')$ levels is given by

$$\beta_r = \frac{A(\Psi J, \Psi' J')}{A_T(\Psi J)} \quad (6)$$

Table 3. Calculated spontaneous emission probabilities, branching ratios and radiative lifetimes for Er^{3+} transitions in CdS -SiO_2 sol-gel glass.

Initial state	**Final state**	**Energy (cm^{-1})**	**$U(2)^2$**	**$U(4)^2$**	**$U(6)^2$**	**A_{ed} (s^{-1})**	**β_r**	**τ_{rad} (μs)**
$^4S_{3/2}$	$^4I_{9/2}$	5956	0	0.0729	0.2560	65.1	0.0324	181
	$^4I_{11/2}$	8251	0	0.0037	0.0789	44.2	0.0220	
	$^4I_{13/2}$	12021	0	0	0.3481	578	0.2879	
	$^4I_{15/2}$	18050	0	0	0.2285	1320	0.6576	
$^2H_{11/2}$	$^4I_{15/2}$	18797	0.0397	0.0807	0.0846	8110	1	138

Table 3 shows the spontaneous transition probabilities, branching ratios and radiative lifetimes for the observed green emissions in Er^{3+} doped CdS -SiO_2 glass. The branching ratios as calculated for these transitions are 65.7 % and 100 % respectively, indicating that green transitions are the main photoluminescence emissions of Er^{3+} in the CdS -SiO_2 glass.

Table 4. Various radiative parameters associated with $^4S_{3/2} \rightarrow {}^4I_{15/2}$ *and* $^2H_{11/2} \rightarrow {}^4I_{15/2}$ Er^{3+} *transitions in CdS -*SiO_2 *sol-gel glass.*

Emission transition	**λ (nm)**	**Δ λ (nm)**	**FWHM (nm)**	**τ_{rad} (ms)**	**$\sigma(\lambda_p)$ (10^{-20} cm^2)**	**$\sigma(\lambda_p) x \tau_{rad}$ ($10^{-24} cm^2 s$)**	**$\Sigma(\lambda_p)$ x FWHM ($10^{-26} cm^3$)**
$^4S_{3/2} \rightarrow {}^4I_{15/2}$	549	11.57	32.75	181	0.545	0.9867	1.785
$^2H_{11/2} \rightarrow {}^4I_{15/2}$	533	7.50	15.67	138	4.52	6.2421	7.0857

Other important radiative parameters associated with the green emission bands for the studied glass are compiled in Table 4. Transitions having spontaneous emission probability greater than $500 s^{-1}$, fluorescence branching ratio ~ 0.5 and ~ 6000 cm^{-1} of energy separation between the energy level under consideration and terminating level are considered to be good radiative transitions [36]. The last requirement is generally essential in order to circumvent the nonradiative rates [37]. The spontaneous emission probability, branching ratio and the energy separation obtained for $^4S_{3/2} \rightarrow {}^4I_{15/2}$ transition in CdS -SiO_2 glass is respectively $1320 s^{-1}$, 0.6576, 18050 cm^{-1} whereas for the $^2H_{11/2} \rightarrow {}^4I_{15/2}$ transition, the corresponding quantities are 8110 s^{-1}, 1.0 and 18797 cm^{-1}; indicates that both the transitions represent potential radiative transitions. Moreover, the radiative lifetimes for the $^4S_{3/2} \rightarrow {}^4I_{15/2}$ and $^2H_{11/2} \rightarrow {}^4I_{15/2}$ transitions in the CdS -SiO_2 glass is 181 and 138 μs respectively. Reasonably higher values of radiative lifetime and stimulated emission cross sections enable them to use as electroluminescent devices in the display technology [37, 38].

The product of peak stimulated emission cross section $\sigma(\lambda_p)$ and radiative lifetime (τ_{rad}) for a particular radiative transition is known as figure of merit for gain and also is a measure of laser threshold whereas large Full Width Half Maxima (FWHM) and $\sigma(\lambda_p)$ are attractive features for broad bandwidth, high gain and low threshold applications [37, 39, 40]. The product $\sigma(\lambda_p) \times \tau_{rad}$ for $^4S_{3/2}$ and $^2H_{11/2}$ manifold of Er^{3+} for the present glass is $\sim 0.986693 \times 10^{-24}$ $cm^2 s$ and 6.24209×10^{-24} $cm^2 s$ respectively. The values are quite comparable with the values reported for soda lime silicate and fluoride glasses [37, 41]. The values of the product $\sigma(\lambda_p) \times$ FWHM is obtained to be $\sim 1.78508 \times 10^{-26}$ and 7.08573×10^{-26} cm^3 for the $^4S_{3/2}$ and $^2H_{11/2}$ manifold respectively. These values are quite high in comparison with other silicate and phosphate glasses [37, 42, 43] indicating that the present glass system will also be suitable for broadband fiber amplifiers.

3.3. Visible upconversion fluorescence

Fig. 3 illustrates the room temperature upconversion spectrum for Er^{3+} doped in CdS -SiO_2 glass under 800 nm excitation. Two intense green emission bands around 533 and 549 nm and a weak red emission band around 626 nm are observed which are attributed to the $^2H_{11/2} \rightarrow {}^4I_{15/2}$, $^4S_{3/2} \rightarrow {}^4I_{15/2}$ and $^4F_{9/2} \rightarrow {}^4I_{15/2}$ Erbium transitions. Two possible mechanisms, namely excited state absorption (ESA) and CR have been proposed to explain the observed upconversion phenomenon.

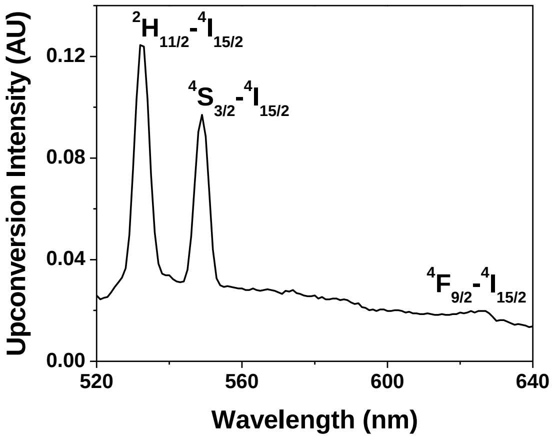

Fig. 3. Upconversion emission spectrum for 0.01M Er^{3+} *doped CdS -*SiO_2 *glass showing intense green emissions under 800 nm excitation.*

According to the energy matching, the possible upconversion mechanism for the emission bands are discussed based on the simplified energy levels of Er^{3+} as presented in Fig. 4.

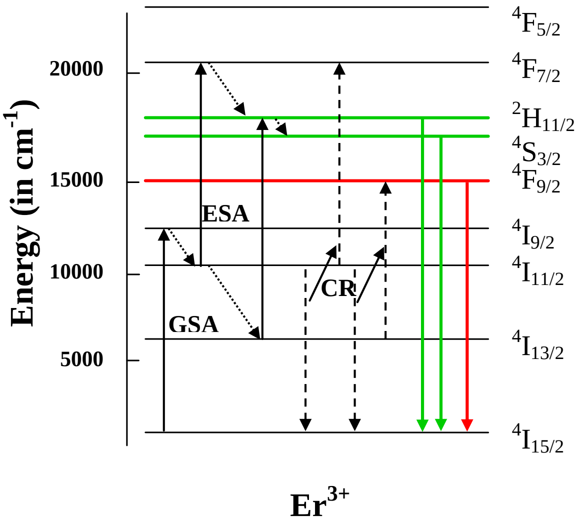

Fig. 4. Energy level scheme for Er^{3+} *ions in CdS -*SiO_2 *sol-gel glass indicating possible upconversion excitation mechanisms.*

For the green emissions, in the first step the input radiation of 800 nm along with phonon excitation will populate the $^4I_{9/2}$ level. The excited energy that stores in the $^4I_{9/2}$ level then relaxes non-radiatively to the $^4I_{11/2}$ and $^4I_{13/2}$ levels. Part of the excitation energy in the $^4I_{11/2}$ level relaxes further radiatively and non-radiatively to the $^4I_{13/2}$ level owing to the small energy gap between them. The second step involves the excitation processes based on the long-lived $^4I_{11/2}$ and $^4I_{13/2}$ levels as follows.

CR, $^4I_{11/2}\,(Er^{3+}) + {}^4I_{11/2}\,(Er^{3+}) \rightarrow {}^4F_{7/2}\,(Er^{3+}) + {}^4I_{15/2}\,(Er^{3+})$
$^4I_{11/2}\,(Er^{3+}) + {}^4I_{13/2}\,(Er^{3+}) \rightarrow {}^4F_{9/2}\,(Er^{3+}) + {}^4I_{15/2}\,(Er^{3+})$
ESA, $^4I_{11/2}\,(Er^{3+})$ + a photon $\rightarrow {}^4F_{7/2}\,(Er^{3+})$
$^4I_{13/2}\,(Er^{3+})$ + a photon $\rightarrow {}^2H_{11/2}\,(Er^{3+})$

The populated $^4F_{7/2}$ level then relaxes rapidly and nonradiatively to the next lower levels $^2H_{11/2}$ and $^4S_{3/2}$. Under this excitation condition, the excited state absorption (ESA) process from the $^4I_{13/2}$ level to the $^2H_{11/2}$ level can also occur more easily. The CR through the $^4I_{11/2}$ level and the ESA from the $^4I_{11/2}$ level should also be considered, but the contributions are much smaller than ESA from the $^4I_{13/2}$ level [44]. Er^{3+} ion at the $^2H_{11/2}$ state can also decay to the $^4S_{3/2}$ state due to multiphonon relaxation process as the estimated energy gap between the $^2H_{11/2}$ state and the next lower state $^4S_{3/2}$ is only 800 cm^{-1} [45]. The above processes populate the $^2H_{11/2}$ and $^4S_{3/2}$ states and the radiative relaxation from these states to the ground $^4I_{15/2}$ state produces green emissions centered at 533 and 549 nm, respectively. The red emission at 626nm is originated from the $^4F_{9/2} \rightarrow {}^4I_{15/2}$ transition and the population of $^4F_{9/2}$ is mainly because of CR from the $^4I_{13/2}$ level plus a small contribution from the higher energy levels ($^2H_{11/2}$ and $^4S_{3/2}$) via non-radiative relaxation. The CR process can be represented as

CR, $^4I_{13/2}\,(Er^{3+}) + {}^4I_{11/2}\,(Er^{3+}) \rightarrow {}^4F_{9/2}\,(Er^{3+}) + {}^4I_{15/2}\,(Er^{3+})$

and it is the dominant contribution for the red upconversion.

The ratio of radiation energies for the two emission bands can be described by the ratio of emission intensities integrated along wave number ν [25], i.e.

$$\int_{\nu_1}^{\nu_2} \rho_{red}(\nu)\,d\nu : \int_{\nu_1'}^{\nu_2'} \rho_{green}(\nu)\,d\nu = \int_{\nu_1}^{\nu_2} I_{red}(\nu)\,d\nu : \int_{\nu_1'}^{\nu_2'} I_{green}(\nu)\,d\nu \quad (7)$$

where $\rho(\nu)$ is the energy density. The calculated integrated intensity $\int I(\nu)d\nu$ ratio between the red and green bands from the observed upconversion spectrum is ~ 1: 122. The results show that the 533 nm and 549 nm green emission bands occupy about 99 % of the total emitted energy in the studied glass sample. Moreover, the calculated integrated intensity ratio between the green emission bands in upconversion to that in fluorescence is observed to be ~ 1:31.

It is a well known fact that the absorption and fluorescence intensity of rare earths (RE) doped in glasses depend strongly on the network formers and network modifiers. Our study shows that Er^{3+} doped with CdS possess very efficient green photoluminescence and up-conversion. We attribute this result to the change in structural features of the glass network because of the addition of CdS [46]. Yang et al. [47] also proposed an explanation that the doping of CdS can increase concentration of Si dangling bonds and oxygen vacancy in the network of the silica xerogel. This means that CdS is thought to introduce non-bridging oxygens (NBOs) into the mix, which are oxygens that form only one bond with silica, leaving another open to bond with a RE. In this way, CdS surrounds each Erbium ion, distancing each ion from the other. This in turn reduces cross-relaxation and increases fluorescence.

4. Conclusions

The Er^{3+} doped in CdS -SiO_2 sol-gel glass is studied for its use as efficient optical material. Judd Ofelt intensity parameters indicate the worth of the present glass host for efficient optical transitions. Strong green fluorescence and upconversion emissions along with estimated branching ratios suggest a potential laser transition for Er^{3+} ions at 533 and 549 nm in the investigated glass.

Acknowledgements

The author acknowledges Govt. of Assam for Special Assistance Grant and UGC-SAP DRS. Author would also like to thank Dr S. Rai, Associate Professor, Department of Physics, Dibrugarh University for fruitful discussions.

References

[1] M. J. Weber, J.Non-Cryst Solids. **123**, 208 (1990).
[2] A. V. Kiryanov, V. Aboites, A. M. Belobolov, M. J. Damsel, A. Minasian, M. I. Timoshechkin, M. I. Belobolov, J. Lumin. **715**, 102 (2003).
[3] W. J. Minisealeo, R. S. Quimbly, Opt. Lett. **16**, 258 (1991).
[4] J. Heo, Y. B. Shin, J. N. Jang, Appl. Opt. **34**, 4284 (1995).
[5] R. Y. Hu, S. Jiang, G. Sorbello, T. Luo, Y. Ding, B. C. Hwang, J. H. Kim, H. J. Seo, N. Peyghambarian, J. Opt. Soc. Am B **18**, 1928 (2001).
[6] S. R. Elliott, Physics of Amorphous Materials, Section 3, Longman Science and Technology, Essex, (1990).
[7] V. Ravi Kumar, M. Rami Reddy, N. Veeraiah, Phys. Stat. Sol. (a) **147**, 601 (1995).
[8] A. V. Ravi Kumar, B. Appa Rao, N. Veeraiah, Mater. Res. Bull. **21**, 341 (1998).
[9] D. Chen, Y. Wang, E. Ma, F. Bao, Y. Yu, Scripta Materialia **55**, 891 (2006).
[10] N. Chiodini, A.paleari, G. Brambilla, E. R. Taylor, Appl. Phys. Lett. **80**, 4449 (2002).
[11] A. C. Yanes, J. Del Castillo, M. Torres, J. Peraza, V. D. Rodriguez, J. Mendez-Ramos, Appl. Phys.

Lett. **85**, 2343 (2004).
[12] J. Bang, H. Yang, P. H. Holloway, J. Chem. Phys. **123**, 084709 (2005).
[13] M. Nogami, T. Enomoto, T. Hayakawa, J. Lumin. **97**, 147 (2002).
[14] S. T. Selvan, T. Hayakawa, M. Nogami J. Non-Cryst. Solids. **291**,137 (2001).
[15] P. V. Jyothy, K. A. Amreetha, J. Gijo, N. V. Unnikrishnan, J. Fluoresce. **19**, 19 (2009).
[16] J. Mu, L. Xu, X. Li, Z. Xu, Q. Wei, H. Sun, S. Kang, J. Dispersion Sci.Tech. **27**(2), 235 (2006).
[17] P. Dutta, S. Rai, Met. Mater. Process. **20**(3), 221 (2008).
[18] P. Dutta, S. Rai, Optik. **122**, 858 (2011).
[19] B. R. Judd, Phys. Rev. **127**, 750 (1962).
[20] G. S. Ofelt, J. Chem. Phys. **37**, 511 (1962).
[21] Z. Suling, H. Yanbing, S. Li, X. Xurong, J. Alloys and Compounds. **31**, 57 (2000).
[22] W. T. Carnall, P. R Fields, K. Rajnak, J. Chem. Phys. **49**, 4424 (1968).
[23] G. H. Dieke, Advances in Quantum Electronics, J R Singer (Eds), Columbia University Press, New York, (1961).
[24] M. Eyal, E. Greenberg, R. Reisfeld, N. Spector, Chem. Phys. Lett. **117**, 108 (1985).
[25] Y. M. Yang, B. Q. Yao, B. J. Chen, C. Wang, G. Z. Ren, X. J. Wang, Opt. Mater. **29**, 1159 (2007).
[26] S. B. Rai, Spectrochim. Acta. Part A. **58**, 1559 (2002).
[27] R. R. Reddy, Y. N. Ahammed, P. A. Azeem, K. R. Gopal, T. V. Rao, S. Buddhudu, N. S. Hussain, J. Quant. Spectrose. Radiat. Transf. **77**, 149 (2003).
[28] X. Zou, T. Izumitani, J. Non-Cryst. Solids **162**, 68 (1993).
[29] X. Qiao, X. Fan, J. Wang, M. Wang, J. Appl. Phys. **99**, 074302 (2006).
[30] X. Zou, T. Izumitani, J. Non-Cryst. Solids. **162**, 68 (1993).
[31] X. Feng, S. Tanabe, T. Hanada, J. Am. Ceram. Soc. **84**, 165 (2001).
[32] H. Lin, E. Y. B. Pun, S. Q. Man, K. R. Liu, J. Opt. Soc. Am. B. **18**, 602 (2001).
[33] S. Tanabe, N. Sugimoto, S. Ito, T. Hanada, J. Lumin. **87-89**, 670 (2000).
[34] A. A. Kaminskii, Laser Crystals: Their Physics and Properties, 4th ed., Springer-Verlag, New York, (1996).
[35] C. Guery, J. L. Adam, J. Lucas, J. Lumin. **42**, 181 (1988).
[36] C. K. Jørgensen, R. Reisfeld, J. Less-Common Met. **93**, 107 (1983).
[37] Y. K. Sharma, S. S. L. Surana, R. K. Singh, R. P. Dubedi, Opt. Mater. **29**, 598 (2007).
[38] A. R. Zanatta, L. A. Nunes, Appl. Phys. Lett. **72**, 3127 (1998).
[39] M. Naftaly, A. Jha, J. Appl. Phys. **87**, 2098 (2000).
[40] S. S. L. Surana, Y. K. Sharma, S. P. Tendon, Mater. Sci. Eng. B. **83**, 204 (2001).
[41] S. Ronchin, R. Rolli, M. Montagna, C. Duverger, V. Tikhomirov, A. Jha, M. Ferrari, G. C. Righini, S. Pelli, M. Fossi, J. Non-Cryst.Solids. **289**, 243 (2001).
[42] J. Yang, S. Dai, Y. Zhou, L. Wen, H. Lu, Z. Ziang, J. Appl. Phys. **93**, 977 (2003).
[43] H. Yanagita, K. Okada, K. Miura, H. Toratani, T. Yamashita, Mater. Sci. Forum. **67&68**, 521 (1991).
[44] H. Lin, E. Y. B. Pun, X. R. Liu, J. Non-Cryst. Solids. **283**, 27 (2001).
[45] S. Q. Man, E. Y. B. Pun, P. S. Chung, Appl. Phys. Lett. **77**, 483 (2000).
[46] S. T. Selvan, T. Hayakawa, M. Nogami, J. Phys. Chem. B. **103**, 7064 (1999).
[47] P. Yang, C. F Song, M. K. Lu, X. Yin, G. J. Zhou, D. Xu, D. R. Yuan, Chem. Phys. Lett. **345**, 429 (2001).

---

[*] Corresponding author: dutta.pankaj@rediffmail.com